ARL-TR-9418 • MAR 2022

DEVCOM ARMY RESEARCH LABORATORY

Understanding Blue Whirl Combustion for Fuel-Flexible Energy Extraction (Summary Technical Report, Mar 2019–Apr 2021)

by Paul M Anderson

NOTICES

Disclaimers

The findings in this report are not to be construed as an official Department of the Army position unless so designated by other authorized documents.

Citation of manufacturer's or trade names does not constitute an official endorsement or approval of the use thereof.

Destroy this report when it is no longer needed. Do not return it to the originator.

ARL-TR-9418 ● MAR 2022

Understanding Blue Whirl Combustion for Fuel-Flexible Energy Extraction (Summary Technical Report, Mar 2019–Apr 2021)

Paul M Anderson
DEVCOM Army Research Laboratory

REPORT DOCUMENTATION PAGE

Form Approved
OMB No. 0704-0188

1. REPORT DATE *(DD-MM-YYYY)*	2. REPORT TYPE	3. DATES COVERED (From - To)
March 2022	Summary Technical Report	1 March 2019–30 April 2021

4. TITLE AND SUBTITLE
Understanding Blue Whirl Combustion for Fuel-Flexible Energy Extraction (Summary Technical Report, Mar 2019–Apr 2021)

5a. CONTRACT NUMBER

5b. GRANT NUMBER

5c. PROGRAM ELEMENT NUMBER

6. AUTHOR(S)
Paul M Anderson

5d. PROJECT NUMBER

5e. TASK NUMBER

5f. WORK UNIT NUMBER

7. PERFORMING ORGANIZATION NAME(S) AND ADDRESS(ES)
DEVCOM Army Research Laboratory
ATTN: FCDD-RLS-CC
2800 Powder Mill Rd
Adelphi, MD 20783-1138

8. PERFORMING ORGANIZATION REPORT NUMBER
ARL-TR-9418

9. SPONSORING/MONITORING AGENCY NAME(S) AND ADDRESS(ES)

10. SPONSOR/MONITOR'S ACRONYM(S)

11. SPONSOR/MONITOR'S REPORT NUMBER(S)

12. DISTRIBUTION/AVAILABILITY STATEMENT
Approved for public release: distribution unlimited.

13. SUPPLEMENTARY NOTES

14. ABSTRACT
This work examines the physical underpinnings of the blue whirl: a new regime of soot-free combustion evolving naturally from fire whirls across a broad range of fuels and having potential as a fuel-flexible heat source for power generation. Experiments found blue whirl formation to depend more on fluid dynamics than chemical kinetics and requires both vortex-generating and surface airflows. Successful simulation of the blue whirl revealed a bubble-mode vortex breakdown flow structure and the presence of three distinct flame types. This structure persisted in simulations in which the flame was rotated up to 15° with respect to gravity, indicating dominance of rotational over axial inertial forces. An advanced experimental burner was designed and constructed, providing control over airflow rates, profiles and temperatures, fuel delivery, and burner height and diameter. Blue whirls produced with the burner could be sustained indefinitely, and flame stability with respect to radial and tangential airflow rates, fuel type, and fuel flow rates was mapped. Stable blue whirls were formed across a wide range of conditions, reaching heat release rates exceeding 750 W. Analysis found that the blue whirl resides in a non-dimensional parameter space sufficiently dominated by rotational airflow below the onset of turbulence.

15. SUBJECT TERMS
STR, combustion, multi-fuel, vortex breakdown, laminar flames

16. SECURITY CLASSIFICATION OF:			17. LIMITATION OF ABSTRACT	18. NUMBER OF PAGES	19a. NAME OF RESPONSIBLE PERSON
a. REPORT	b. ABSTRACT	c. THIS PAGE			Paul M Anderson
Unclassified	Unclassified	Unclassified	UU	32	19b. TELEPHONE NUMBER (Include area code) (301) 394-1276

Contents

List of Figures

List of Tables

Executive Summary

The blue whirl is a recently discovered combustion regime possessing desirable traits such as soot-free burning and the ability to ignite across a wide range of fuels without the need for fuel pre-vaporization or atomization. These and other features of the phenomenon make it an intriguing candidate as a heat source for fuel-flexible power generation. Such a technology could broaden the power generation options available to Soldiers, to include use of local or contaminated fuels and biomass-derived fuels in addition to existing logistics fuels. This would have the potential of extending operation range, enhancing energy reliability, and reducing energy logistics burdens for teams employing such a technology.

The present study was performed at the US Army Combat Capabilities Development Command Army Research Laboratory in Adelphi, Maryland, between March 2019 and April 2021 under the Director's Research Awards – Transformative Research Challenge (DIRA-TRC) program. The goal was to advance the development of fuel-flexible combustion technology by better understanding the physical and chemical underpinnings of the blue whirl phenomenon. This was achieved through three tasks: 1) determine the essential ingredients of forming and sustaining blue whirls and explore the role of chemical functionality on blue whirl formation and emissions; 2) numerically simulate the blue whirl to probe its structure as well as its behavior under non-experimentally testable conditions of interest; and 3) construct an advanced burner with greater control over experimental parameters to find the stability limits of the blue whirl, optimize fuel and airflow rates, understand how the blue whirl scales, and inform the design of a future prototype.

Task 1 experiments uncovered two separate airflows critical to the formation and stability of the blue whirl: one tangential to the flame that generates the vortex flow and one that approaches the flame radially along the bottom boundary of the burner. The blue whirl's existence depends on the ratio and magnitudes of these flows. These experiments also confirmed the soot-free nature of the blue whirl and indicated that it is governed more by fluid dynamics and fuel thermophysical properties than by reaction kinetics. This latter result simplified subsequent modeling efforts by justifying the use of single-step chemistry.

Task 2 efforts to numerically model the blue whirl were successful, revealing a flow structure known as bubble-mode vortex breakdown and a mixing structure combining three distinct flame regimes. Blue whirl structure was found in simulations to be unaffected by rotating the burner up to 15° with respect to gravity. This suggests that the blue whirl is strongly dominated by rotational rather than

axial flow and indicates that a blue whirl-based technology would be robust against changing orientations encountered in the field.

An advanced burner was designed and constructed in Task 3, giving control over airflow rates, profiles and temperatures, burner height and diameter, and fuel delivery. Blue whirls produced with the apparatus could be sustained indefinitely, so long as fuel and air were supplied, and maps of blue whirl stability with respect to radial and tangential airflow rates, fuel type, and fuel flow rates were developed. By tuning air and fuel flow rates, stable blue whirls were formed across a broad range of conditions, reaching a maximum heat release rate of 750 W—nearly 4 times that which had been previously reported. Analysis found that the blue whirl resides in a non-dimensional parameter space sufficiently dominated by rotational airflow without inducing turbulence.

There were no results that contraindicate the blue whirl as the basis for a fuel-flexible energy conversion technology. Key advances in favor of its potential in this regard were the ability to sustain blue whirl flames indefinitely and across a broad range of fuels, an increase in thermal output up to 750 W, and robust stability with respect to changing burner orientations. Recommended future efforts should focus on understanding fuel evaporation processes in the blue whirl as this is essential to harnessing flexibility with real fuels and in determining power-to-volume limits. The advanced burner developed here can be exploited to examine both questions.

1. Introduction

Liquid hydrocarbon fuels are an eminently practical energy source for the US Army. They are energy dense, portable, and used in established technologies that are well understood and reliable. Unfortunately, these technologies are also fuel-specific and require fuels meeting narrow composition tolerances.[1,2] At the same time, the Maneuver Center of Excellence has stated the need to develop more persistent power and energy availability for emerging expeditionary Brigade Combat Teams operations such as manned and unmanned teaming. These unmanned autonomous systems are short-lived because of limited logistics supply of batteries or JP-8. A single technology capable of extracting energy from a wide range of liquid fuels, including those derived from local resources, would therefore be of extraordinary benefit. It could extend the range and endurance of autonomous systems in Multi-Domain Operations, improve energy security, and reduce energy logistics costs. The recently discovered phenomenon known as blue whirl combustion has the potential to form the basis for such a technology. The work detailed in the present report represents the US Army's first attempt to investigate blue whirl combustion for this purpose. Funding was provided through the US Army Combat Capabilities Development Command Army Research Laboratory's Director's Research Awards – Transformative Research Challenge (DIRA-TRC) program, and the period of performance was from March 2019 through April 2021.

The blue whirl was unexpectedly discovered in 2016 by Xiao and coworkers at the University of Maryland while investigating the use of fire whirls for oil spill remediation.[3] Their experiment used an eddy-producing enclosure comprising two quartz half shells offset to produce a tangential entrainment of air. A conventional fire whirl that formed from air buoyantly drawn into the enclosure spontaneously developed into a blue whirl when the liquid fuel was deposited on a water surface that permitted unobstructed surface airflow. Blue whirl formation was found to occur in three stages, as shown in Fig. 1. It begins with the ignition of a pool of liquid fuel that quickly forms into a fire whirl. This is followed by a transitional whirl that still possesses luminous soot, but also displays a blue structure at its base and rotates more vigorously than the fire whirl. The transitional whirl then shrinks to a small blue whirl, which may burn steadily or may oscillate to and from the transitional whirl, depending on test conditions. The blue whirl is a small and stable flame that appears as an inverted blue cone, with the blue color indicating soot-free combustion. Moreover, the researchers observed that a blue whirl could be formed from a variety of fuels including n-heptane, n-octane, ethanol, and even crude oil.

Fig. 1 The three stages of blue whirl formation: (left to right) fire whirl, transitional whirl, and blue whirl

Researchers at the DEVCOM Army Research Laboratory recognized that the blue whirl possessed characteristics that could translate into technologies with beneficial features for the Warfighter. Table 1 summarizes these observations.

Table 1 Observed blue whirl characteristics with potential technologies and their impacts

Observation	Potential technology	Potential impact
• Complete combustion across range of fuels • No atomization or pre-vaporization • Formation despite water	• Efficient fuel usage • Fuel flexibility for use of converted biomass and captured or scavenged fuel	• Extend operation range • On-demand energy at point of need • Reduce energy logistic costs
• Experimentally simple • Buoyancy-induced flows at 1 atm • Wide tolerance burner construction	• Robust, reliable, low maintenance • Low acoustic signature • Many options for manufacture	• Extend operation range • Greater power generation reliability • Surveillance capability • Low-cost, on-demand production
• Blue flame—soot-free combustion	• No soot catalysts needed • Minimal radiative heat load • No soot fouling	• Minimize health and environmental impacts • Compact, simpler, lighter, more-reliable power generation

There were three facets to DEVCOM ARL's investigation of the blue whirl and its potential as a fuel-flexible combustion technology:

Task 1. Experiment with a passive, fixed-frame apparatus to

- Identify key ingredients in forming and sustaining blue whirls.
- Learn the role of fuel characteristics on blue whirl creation and emissions.
- Inform the development of models and an advanced experimental burner.

Task 2. Develop computer simulations of the blue whirl to

- Further reveal fundamental blue whirl structure.
- Test conditions difficult to probe with experiments.

Task 3. Construct and experiment with an advanced experimental burner with greater control of test conditions to

- Quantify the blue whirl's stability limits across a range of key parameters.
- Help validate models.
- Find conditions that increase fuel flexibility and/or flame stability.
- Determine scaling with heat release rate.
- Inform the future design of a practical burner prototype.

2. Methods/Results

2.1 Task 1: Fixed Frame Experiments

2.1.1 Methods

The key elements of Task 1 are presented here. For additional details and relevant literature, the reader is referred to our publication in *Energy & Fuels*.[4] The experimental apparatus employed for Task 1 enabled us to reproduce and extend beyond the results of prior researchers. The apparatus, shown in Fig. 2, comprised two quartz half shells, each 30 cm in diameter, suspended on a fixed frame over an aluminum plate with a centrally located fuel port. The aluminum plate was selected as a more application-practical burning surface than the water surface used in previous studies; however, a flow of water on the underside of the plate could still be used to regulate the plate temperature. This control was included because greater instability was observed in blue whirls formed over an aluminum plate than over water, similar to Hariharan et al.[5] However, no difference was seen once water flow was present to regulate plate temperature. This suggests that the water chiefly serves as a thermal mass that mitigates hot spots on the aluminum surface that would otherwise cause fuel to evaporate in regions separated from the blue whirl's thermal feedback mechanism.

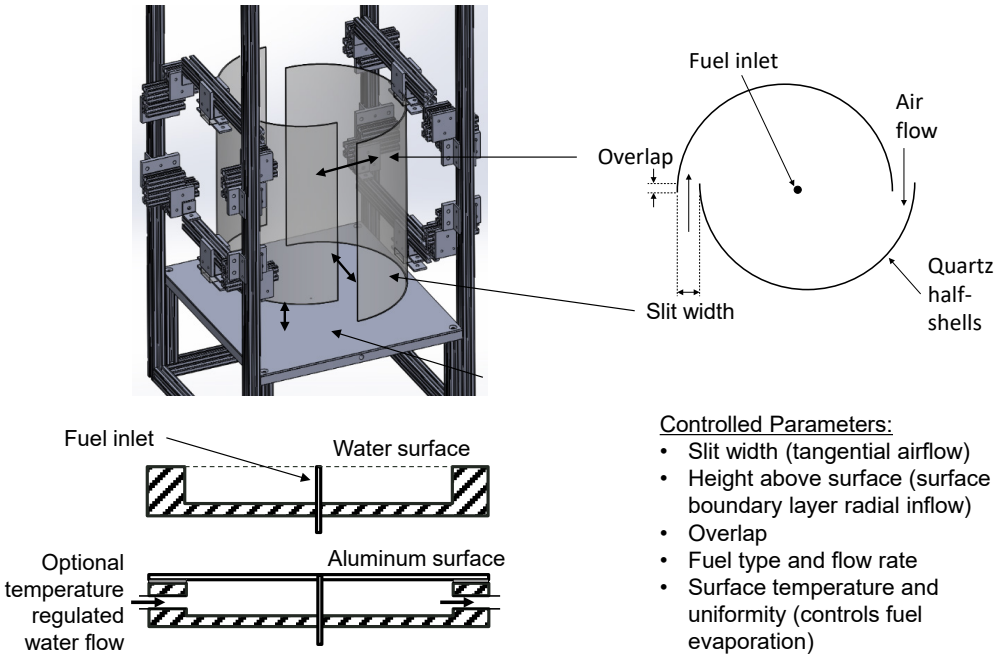

Fig. 2 Fixed-frame blue whirl apparatus used in Task 1

The configuration of the quartz cylindrical half shells dictated how air was entrained into the enclosure. A slit of width *w*, created by the offset of the quartz half shells, induced a vortex flow in the naturally entrained air. Raising the half shells a height *h* above the plate allowed air to be drawn in radially along the plate surface. While vortex flow of fuel and air mixtures is a common feature of many combustors, an unrestricted radial boundary layer flow is unique to this experimental configuration.

The steps to generate a blue whirl with this apparatus were the same regardless of the fuel used. Fuel was first pumped to the aluminum surface until a pool large enough to support a large fire whirl accumulated (about 8 mL). The pool was ignited manually with a lighter, and this quickly developed into a fire whirl, which shrunk as fuel was consumed, until it transitioned into a blue whirl. The blue whirl was maintained by matching the fuel flow rate with the burning rate.

2.1.2 Results

Blue whirl stability was measured as the average duration in which the blue whirl structure was maintained. To assess the effect of burner configuration and, therefore, airflows on blue whirl stability, parameters *w* and *h* were systematically varied between 5−40 and 0−8 mm, respectively. Having observed a reduction in stability for very large overlap (i.e., high eccentricity) and negative overlap (i.e., a gap across the two half shells), overlap was fixed at 2 mm for all tests. These tests

showed that the greatest blue whirl stability was achieved when the ratio of h/w was between 0.1 and 0.2, which was true regardless of the fuel used. In addition, no stable blue whirl flame could be generated in the absence of radial air inflow along the burning surface, that is, when the value of h was 0. The necessity of this airflow had not been previously reported, although its presence helps explain the inverse cone and lifted flame structure of the blue whirl by way of the Ekman pumping mechanism.[6] Moreover, the peculiarities of an experimental setup that provides for an unobstructed boundary layer flow may help explain why the blue whirl phenomenon was not observed until only recently.

To investigate the influence of impurities on blue whirl formation, methyl acetate was mixed with varying amounts of deionized water up to 10 wt%, which exceeds its room temperature solubility limit of 8.5 wt%. Again, a blue whirl formed for all fuel–water mixtures considered. However, instability did increase with water content. The reduction in stability could be due to suppressed fuel evaporation caused by the higher specific heat of water as well as disturbances in the radial and tangential airflows caused by the accumulation of water on the plate surface.

To assess the impact of chemical functionality on blue whirl formation, a large number of model fuels, possessing a diverse range of functional groups and representative of a variety of fuel production pathways, were tested. For these tests, the ratio h/w was held constant at 0.15. The results are presented in Table 2. Remarkably, a stable blue whirl (defined as a blue whirl structure sustained without interruption for at least 100 s) was observed for every fuel considered. The only alterations in the experimental setup that were needed to achieve this was the slight tuning of the aluminum plate temperature in correlation with the heat of vaporization of the fuel (Table 3).

Table 2 Impact of fuel chemical functionality on blue whirl formation

Fuel	Fuel production pathway	Functional group(s)	Blue whirl?
Ethanol	Biological	Alcohol	Yes
Butanol	Biological	Alcohol	Yes
Acetone	Biological	Ketone	Yes
Methyl acetate	Thermochemical	Carboxylate ester	Yes
Methyl propionate	Biological	Carboxylic acid ester	Yes
Methanol	Thermochemical/catalytic	Alcohol	Yes
Cyclohexane	Petroleum	Cyclic aliphatic hydrocarbon	Yes
n-heptane	Petroleum	Alkane	Yes
n-octane	Petroleum	Alkane	Yes
iso-octane	Petroleum	Alkane	Yes

Table 3 Impact of fuel thermophysical properties on blue whirl formation

Fuel	Fuel temp for blue whirl (°C)	Heat of vaporization (kJ/mol)	Boiling point (°C)
methyl acetate	15	33	56.8
n-heptane	26	36	98.4
n-octane	47	41	125.6

The diversity of fuels capable of forming a blue whirl, and the monotonic relationship between blue whirl formation and properties regulating fuel evaporation rate, indicate that the blue whirl is governed less by reaction kinetics than by a combination of fluid dynamics and fuel thermophysical properties. This result informed our approach to Task 2 by suggesting the validity of single-step chemistry, an approach that greatly simplified our modeling efforts.

Lastly, combustion efficiency and emissions were compared for three fuels burning in both fire whirl and blue whirl regimes. The results, given in Table 4, show that both flame types exhibited near-complete combustion. Neither flame type produced measurable NO_x nor unburned hydrocarbons, and the soot output by the blue whirl was almost negligible. However, the fire whirl yielded over 3 orders of magnitude more soot for the hydrocarbon fuels and over 5 times more soot for methyl acetate than the blue whirl. At the same time, the blue whirl exhibited about an order of magnitude more carbon monoxide (CO) than did the fire whirl. This difference in soot and CO production propensities is indicative of the presence of a diffusion flame in the case of the fire whirl, while for the case of the blue whirl, at least some fuel-oxidizer premixture is occurring prior to reaction.[7]

Table 4 Impact of fuel type and flame regime on combustion efficiency and emissions

Fuel	Flame regime	Conversion efficiency	NO_x (ppm) per unit fuel	CO (ppm) per unit fuel	Soot production per unit fuel (a.u.)
methyl acetate	Blue whirl	99.3%	0	23	0
n-heptane	Blue whirl	99.1%	0	61	1
n-octane	Blue whirl	99.4%	0	32	1
methyl acetate	Fire whirl	99.6%	0	4	800
n-heptane	Fire whirl	99.4%	0	6	1200
n-octane	Fire whirl	99.4%	0	7	1260

2.2 Task 2: Modeling the Blue Whirl

2.2.1 Methods

The key elements of Task 2 are presented here. For additional details and relevant literature, the reader is referred to our publications.[8,9] Modeling was performed in

a Cartesian domain measuring 30 cm in each dimension, which matches the diameters of the quartz half shells used in experiments. The walls had no-slip and adiabatic boundary conditions. Evaporation of the fuel was not included in the model. Instead, n-heptane vapor at 371 K was delivered though a port, measuring 0.9 cm in diameter, centered on the bottom plane of the simulated space. Informed by Task 1 results, reactions were modeled as single step and infinitely fast.

Figure 3a displays the computational domain with the air and fuel flows that successfully gave rise to a simulated blue whirl. A vortex was produced by injecting air tangentially along each wall through vertical inlets located at each corner of the enclosure. In addition, air was injected through four horizontally oriented inlets located along the bottom boundary. The necessity of this surface airflow was an insight gained from experiments, which proved essential to a successful blue whirl simulation.

Successfully modeling the blue whirl also required increased resolution in the central region of the domain. As shown in Fig. 3b, the innermost portion of the computational domain required a 0.1465-mm mesh size to capture necessary detail, while closer to the walls, a larger 2.344-mm mesh was sufficient. Computations utilized a new barely implicit correction algorithm for low-Mach-number reactive flows that was developed as part of the blue whirl simulation efforts.[9,10]

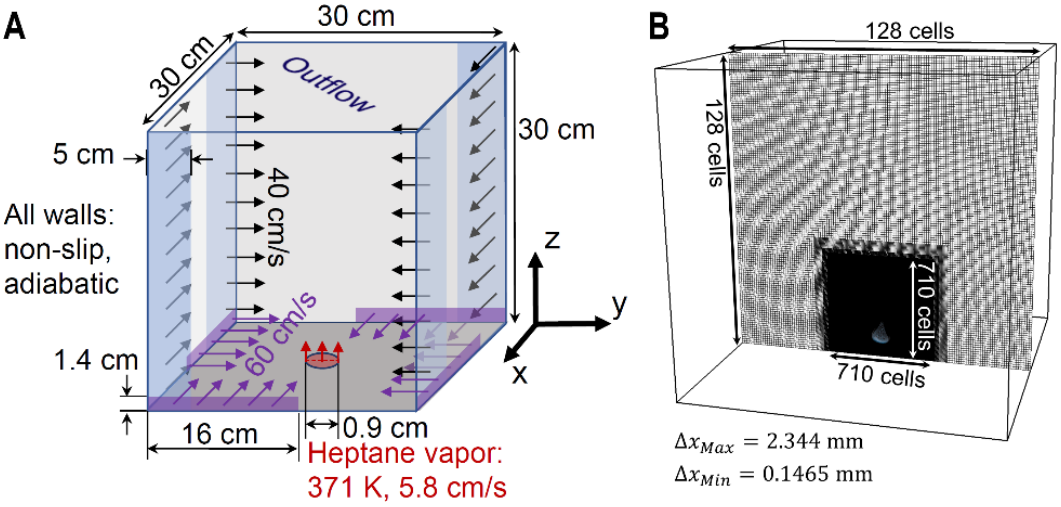

Fig. 3 a) Cartesian computational domain showing the air and fuel flows that successfully modeled a blue whirl flame and b) different mesh sizes used across the domain

2.2.2 Results

The simulated flame structure shown in Fig. 4 reveals three different flame types: a rich premixed flame in the bottom inverted cone, a lean premixed flame in the outer region of the top cone (termed the "purple haze" region), and a diffusion flame

inside the purple haze. All three flame types meet at the triple flame constituting the blue whirl's bright blue rim. The presence of a substantial premixed region is consistent with the emissions observed for the blue whirl in Task 1.

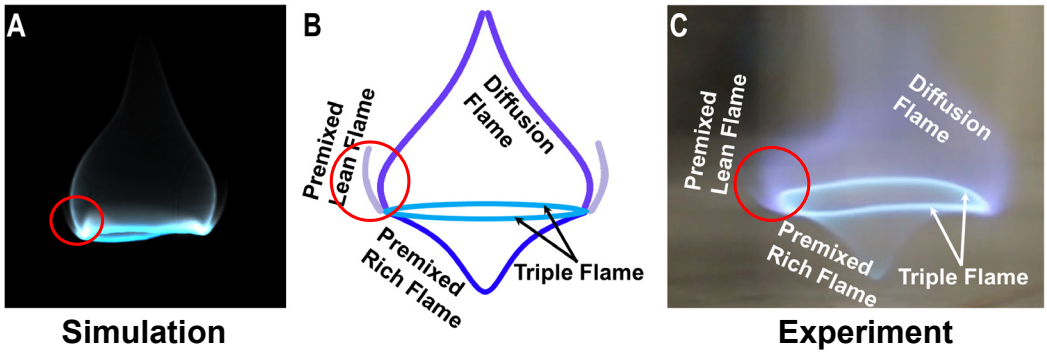

Fig. 4 Flame structure of the blue whirl: a) simulated flame, b) illustrated schematic, and c) image from experiment showing the locations of the different flame types[8]

Simulations also revealed flow structure. Based on observations of a recirculation region made visible by soot streaks during transition from the fire whirl stage (Fig. 5a), it had been hypothesized that the blue whirl was characterized by a bubble-type vortex breakdown.[11] The flow field identified through modeling is consistent with this hypothesis (Fig. 5b). Interestingly, the central recirculation region within the vortex breakdown bubble possesses a structure seen in other combustors designed to induce recirculation. These include trapped vortex (Fig. 5c) and bluff-body combustors (Fig. 5d); however, the blue whirl achieves this structure without walls and other cavity features that can result in the loss of heat and free radicals.[12,13]

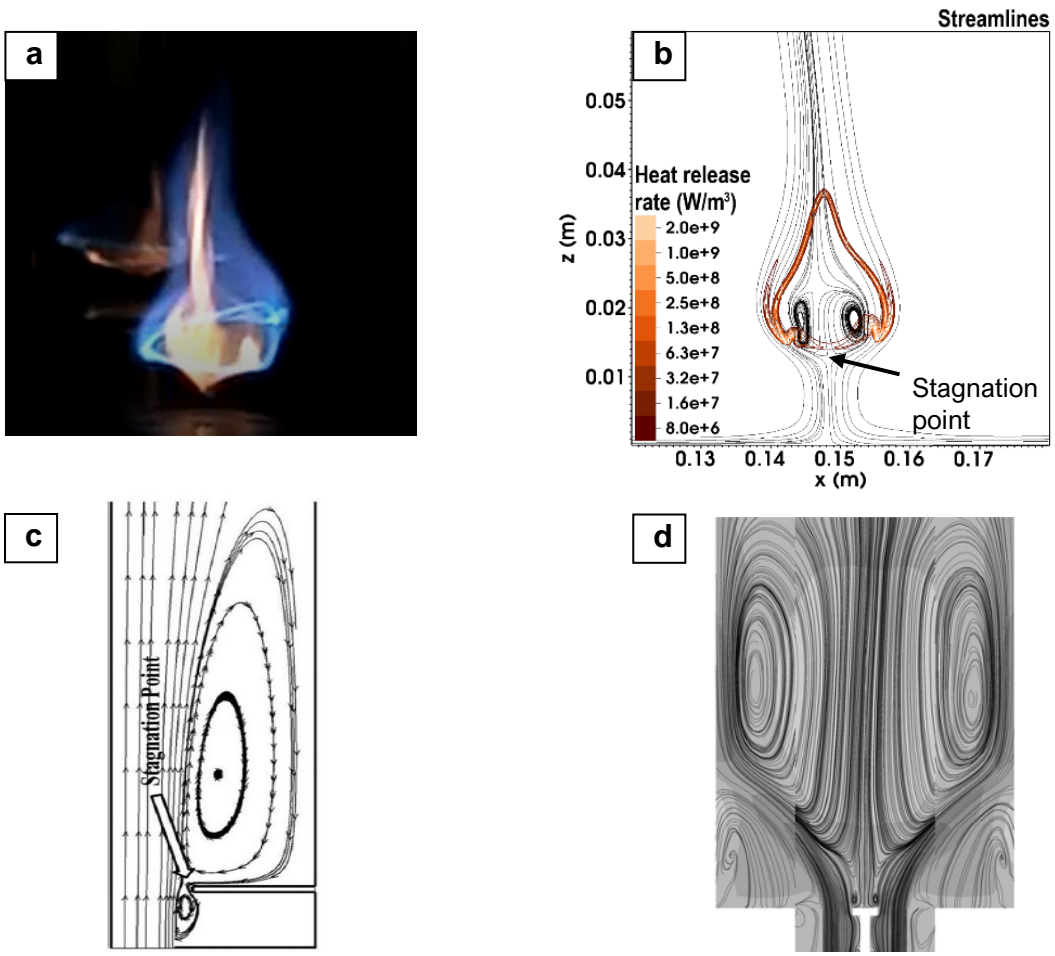

Fig. 5 a) Image capturing visible recirculation during fire whirl to blue whirl transition. b) Streamlines from a center slice of the simulated blue whirl. c) Streamlines of a modeled single-vortex trapped vortex combustor (wake back flow regime).[12] d) Streamlines of a bluff-body stabilized combustor with swirl.[13]

Successful modeling of the blue whirl allowed us to probe additional scenarios of interest that were difficult to examine experimentally. An important question relevant to future applications of a blue whirl-based technology is on the importance of burner orientation: must the blue whirl burner remain horizontal relative to gravity for it to operate? To answer this question, the numerical code was altered to allow for a changing orientation of the gravity vector. The blue whirl was first simulated with the gravity vector pointing normal toward the burner surface until a stable blue whirl was established. Then, in two separate runs, the gravity vector was rotated over a simulated duration of 0.05 real seconds to angles of 5° and 15° with respect to the burner surface. The 15° angle was chosen as a maximum case for a vehicle operating on a steep incline. After rotating the gravity vector, the flame was simulated for an additional 15 s.

The blue whirl remained stable under both tilted conditions, with the overall dynamics matching that of the untilted case. This suggests that the rotational component to the flow dominates over that which is buoyancy-driven. There is some precedent for this behavior in fire whirls, where the flame structure has been experimentally shown to hold up to at least a 30° inclination angle.[14] Figure 6 shows this clearly in a center slice taken at t = 11.3 s for the 15° tilt case. In Fig. 6a, the axial velocities are centered about the flame axis with negligible deviation. In Fig. 6b, we see the tangential velocity at the center slice of the domain overlaid with a volume rendering of heat release rate. Figure 6c gives the radial profiles of circulation for all three tilt angles at the axial locations indicated in Fig. 6b. Circulation is defined as the line integral of tangential velocity along a given circumference. Again, here there is no meaningful difference among the three cases.

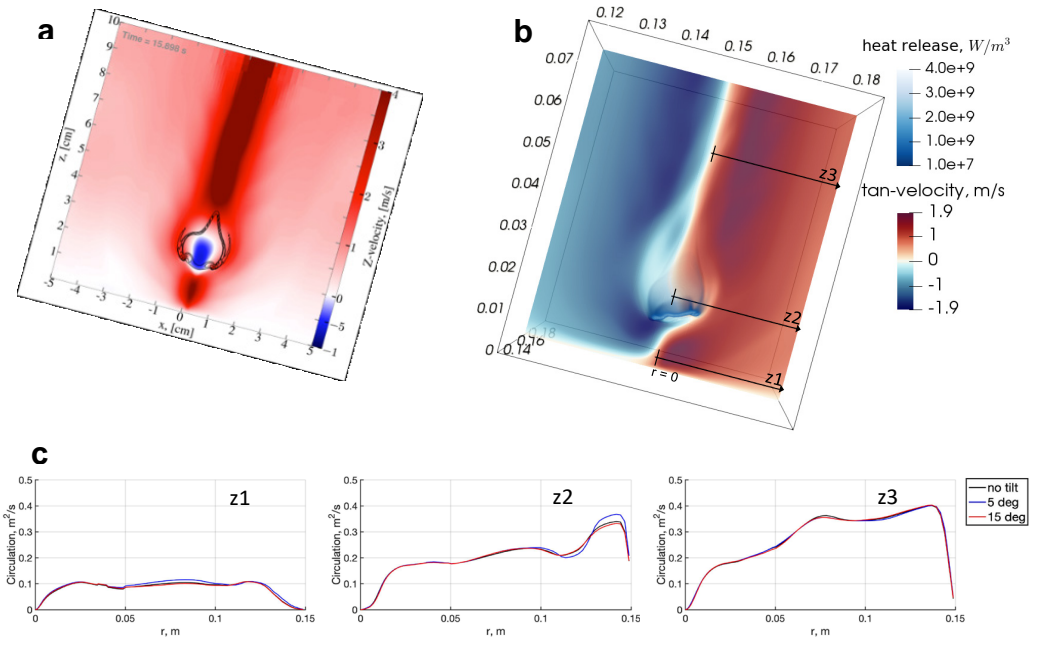

Fig. 6 Simulated blue whirl tilted at 15° with respect to gravity. a) Axial velocity, b) tangential velocity overlaid with a volume rendering of heat release rate, and c) radial circulation profiles for all three tilt angles, 0°, 5°, and 15°, at the axial locations indicated in b).

2.3 Task 3: Advanced Experimental Blue Whirl Burner

2.3.1 Methods

To enable deeper exploration of blue whirl behavior beyond that achievable with the Task 1 apparatus, a new experimental burner was designed and constructed. This apparatus, referred to here as the "advanced burner," provided substantially

greater control over the physical parameters relevant to blue whirl combustion. Its design enables independent control of radial and tangential airflow rates, profiles, and temperatures; control over fuel delivery method, flow rate, and temperature; adjustable burner diameter and height; and visual access across all three spatial dimensions.

The advanced burner, as-designed and as-constructed, is displayed in Fig. 7 (left and middle), respectively. Tangential and radial airflow are independently controlled by way of a double enclosure design, which is most easily seen in Fig. 7 (right). Air delivered to the outer enclosure enters the burner radially (green arrows) along the surface through a 3-mm gap between the burner surface and the bottom of the inner enclosure walls. Air delivered to the inner enclosure enters the burner tangentially (blue arrows) creating a vortex flow. Compressed air from the building is provided to each of the airflow streams, which are each regulated by dedicated airflow controllers. The air temperatures of each airflow could also be increased independently by way of two inline air heaters (Thermal Devices part nos. CBLNA32G10S-26 and CBEN24G6SKHK).

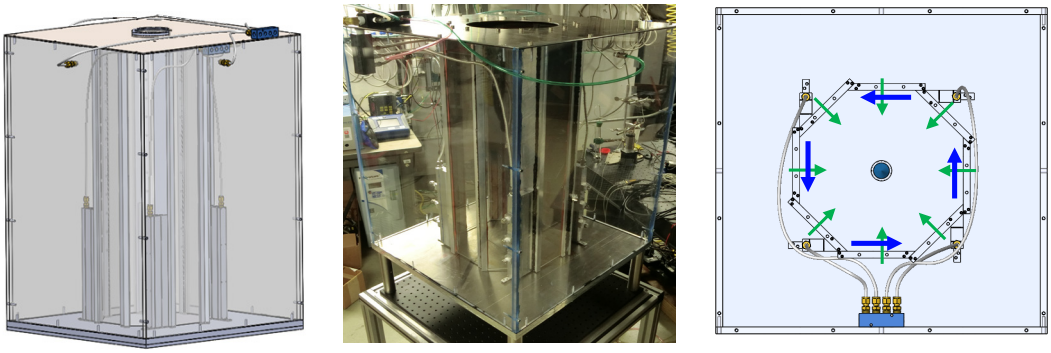

Fig. 7 Advanced experimental blue whirl burner: (left) as-designed and (middle) as-constructed, and (right) top-down schematic showing airflows introduced into the burner chamber radially (green arrows) and tangentially (blue arrows)

The profile of the tangential airflow can also be controlled. Air traveling to each of the four tangential air inlets is first sent through a manifold from which the air is directed to the four ports feeding the inlet assembly, as seen in Fig. 8. Air to each of the four ports is finely controlled by needle valves. The velocity profile resulting from controlling the flow rates to each port was measured on an additional test rig that was identical to the tangential air inlets inside the burner. To make this measurement, a hotwire anemometer mounted to a motor-driven translation stage was passed along the height of the vertically oriented inlet on the test rig.

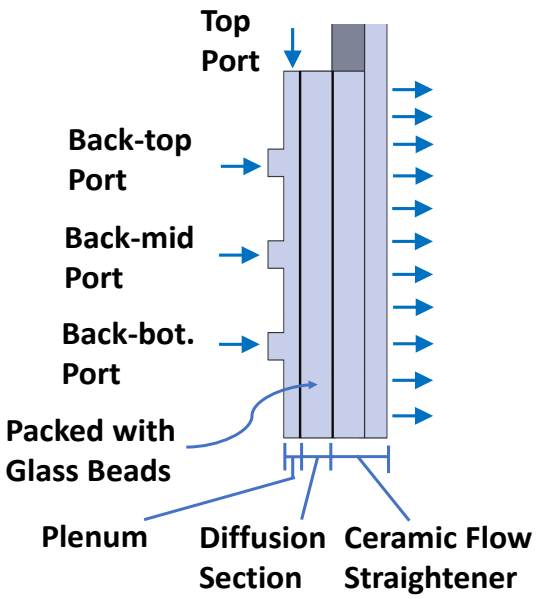

Fig. 8 Tangential air inlet

The outside of the burner has a length, width, and height of 24 × 24 × 30 inches, respectively, and the outer walls are 0.5-inch-thick acrylic. The inner enclosure comprises eight panels that are non-permanently joined together in a regular octagon shape whose inscribed diameter is 30 cm. The panel walls consist of machined aluminum frames inset with quartz glass. The design is such that should laser diagnostics be of future interest, a laser sheet could pass unobstructed through the height of the burner without transmission being altered by any curved surfaces. The octagonal inner enclosure can also be repositioned to create smaller burner diameters. Figure 9 demonstrates how the inner enclosure can shrink and expand similar to a camera iris. Each inner enclosure configuration would require its own unique top plate to which the tops of the wall panels would be affixed. The inner diameter can be reduced to about 6 inches before the tangential airflow inlets begin to impede flame visibility. Likewise, the height of the inner enclosure can be adjusted, as in Fig. 10, by attaching a movable top plate to the tapped mounting holes machined into the inner enclosure. Unfortunately, neither of these size-altering features of the advanced burner were implemented within the time allotted for the current project.

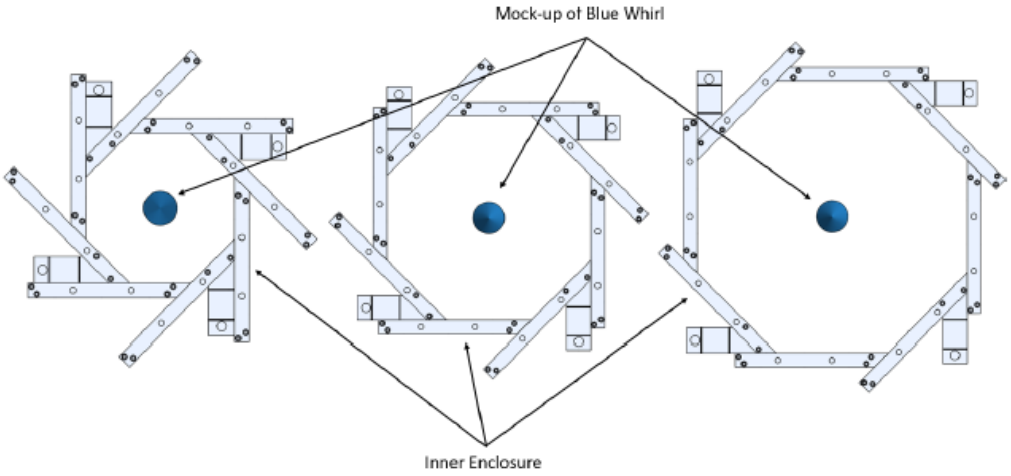

Fig. 9 Inner enclosure can shrink and expand in a camera-iris-like manner, changing the burner chamber diameter

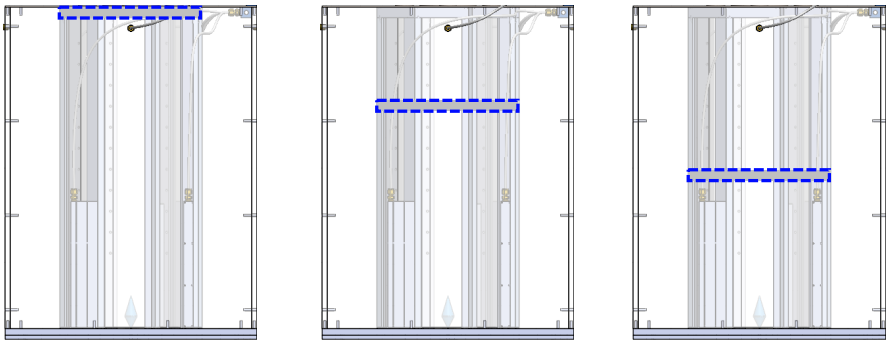

Fig. 10 Burner chamber height can be raised and lowered by attaching a movable top plate

Lastly, fuel is delivered to the center of the burner surface by a Vici M60 positive displacement pump through a 2-mm-diameter port machined into the center of a 1.5-inch-diameter port assembly that is threaded into the bottom surface plate. The removable fuel port assembly allows for different fuel port diameters and configurations, such as an annulus, should there be a desire to test such variations in the future. The fuel pump was calibrated for each fuel tested. To regulate the temperature of the burner surface, water was pumped from a chiller through a cavity beneath the burner surface, as was done with the Task 1 burner (see Fig. 1).

Blue whirls generated with the advanced burner were vastly more stable than those produced by the Task 1 apparatus. Whereas blue whirls produced in the fixed-frame burner were always finite in duration, blue whirls formed in the advanced burner could be sustained indefinitely. Therefore, a new method of flame stability measurement beyond flame longevity needed to be developed. A blue whirl can be readily identified by two key attributes: a lifted vortex rim and the absence of luminous soot. To detect these features, videos of the flame were captured at 24 fps

using a Fastec IL-5 camera (part no. IL5SC81TBD) and then analyzed. For vortex rim identification, images were postprocessed using thresholding and edge detection to define a bounding box encompassing the blue whirl vortex rim. Ideal parameters for these operations were ascertained from a supervised classification machine learning model. The rim was deemed lifted if the bottom of the bounding box was separated from the burner surface in the image. By this method, overall flame stability for a set of test conditions was quantified as the fraction of images possessing a lifted vortex rim. The prevalence of luminous soot was quantified as the average of the image's red channel intensity. Red channel values near their minima corresponded to a blue whirl flame. For additional information regarding image analysis methodology and the design and construction of the advanced burner, the reader is directed to Price.[15]

2.3.2 Results

Experiments with the advanced burner were designed to explore four variables affecting blue whirl stability: tangential air inlet profile, tangential and radial airflow rates, fuel type, and fuel flow rate. Figure 11 shows the tangential air inlet profiles resulting from air being delivered exclusively to each of the three back ports. The plots correspond to a total airflow of 280 slpm delivered to the burner (70 slpm to each inlet); however, the qualitative shapes of each profile hold for all flow rates tested.

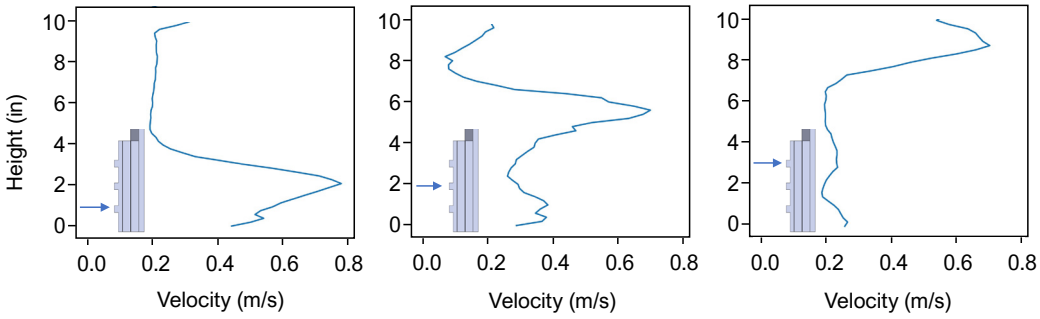

Fig. 11 Tangential airflow velocity profiles for 70 slpm of air delivered exclusively to (from left to right) the back-bottom port, back-middle port, and back-top port of a single tangential air inlet

Figure 12 displays contour plots of blue whirl stability for each airflow profile as tangential and radial airflow rates were varied. The fuel used was n-heptane. Here stability is measured as the fraction of time the flame rim is in a lifted state, with 1.0 representing a perfectly steady blue whirl without any flicker whatsoever and 0.0 representing a flame that never forms a blue whirl. The range of tangential airflows needed to sustain a blue whirl increases with the height of the port used for air delivery, indicating that airflow injected above the height of the blue whirl

has little impact on flame stability. This suggests that the size of a practical device using the blue whirl could be on the order of the flame itself, a relatively small footprint. In contrast to the Task 1 experiments, the blue whirl was able to form without a radially injected airflow; however, its presence did enhance overall stability as well as widen the stability window. Blue whirl stability was poor to the left of the central stable regions in Fig. 12, because there was insufficient airflow to induce the blue whirl structure to form, while to the right of the central region, the blue whirl structure could no longer be maintained due to the onset of turbulence. The region of stability is sloped in the cases of the back-middle and back-top ports. This is likely because in these configurations, the change in air velocity near the burner surface is not linear with respect to overall airflow rate. It is worth noting that for the case of the back-bottom port, the blue whirl is most stable at a radial-to-tangential airflow ratio of 0.25, which is remarkably close to the ratio 0.224, which was used in successful blue whirl simulations (see Fig. 3a).

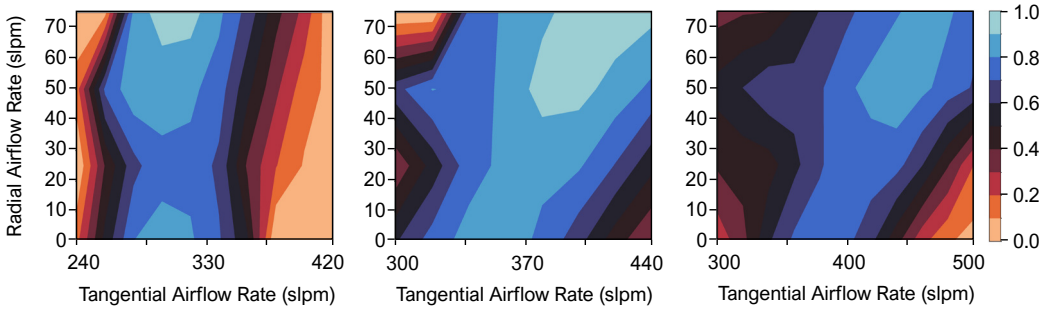

Fig. 12 Blue whirl flame stability for each of the velocity profiles from Fig. 11 as tangential and radial airflows are varied

Using soot luminosity to quantify blue whirl stability produced a result consistent with the lifted rim detection method. Figure 13 plots blue whirl stability using both measurement methods for tangential air delivered to the back-top port. As would be expected, red channel intensity exhibited the inverse response to blue whirl stability. It should be noted that while the soot intensity method of blue whirl detection has the advantage of being computationally simpler, it would not perform well for fuels that do not have a strong sooting propensity, such as many alcohols.

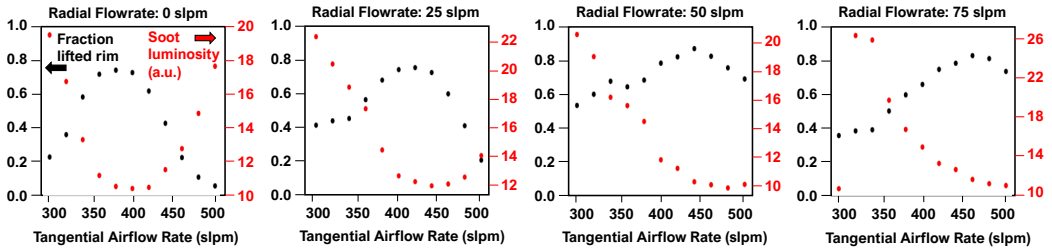

Fig. 13 Blue whirl stability for n-heptane fuel using the back-top tangential air inlet port. Stability increases with the fraction of images exhibiting a lifted rim (black) and decreases with soot luminosity (red).

To test the effect of fuel type on blue whirl stability, n-octane and methyl acetate were chosen alongside n-heptane and run with the tangential airflow in the back-bottom configuration. This is consistent with the fuels selected for emission analysis in Task 1, and in keeping with that experiment, the burner plate temperatures were set to 25, 50, and 15 °C for n-heptane, n-octane, and methyl acetate, respectively. Fuel flow rates were chosen such that each fuel's heat release rate was 360 W (±25 W). From Fig. 14, n-heptane and n-octane showed very similar behaviors in terms of both magnitude and range of stability. However, methyl acetate deviates substantially—the blue whirl was more stable both in terms of the fraction of images exhibiting the signature lifted rim and in the range of radial and tangential airflows producing a stable blue whirl. Indeed, across the sweep of values chosen for the experiment, neither a lower bound for tangential airflow nor an upper bound for radial airflow was reached in which stability began to drop off. This behavior is undoubtedly regulated by evaporation rates; however, it is not readily explained with a simple treatment of the classical Stefan problem applied to fire whirls.[16] A more detailed modeling of fuel evaporation would be needed to explore this effect further; however, this is beyond the scope of this project.

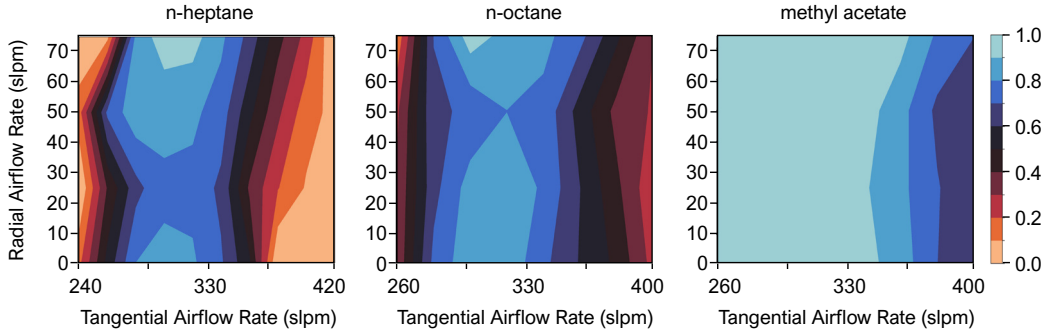

Fig. 14 Blue whirl stability for different fuels

The last variable considered, fuel flow rate, is of particular importance as this dictates the maximum thermal power available for an application. Tests were run

with different flow rates of n-heptane and while varying the tangential airflow rate. The tangential airflow was injected in the back-bottom port configuration. The radial airflow rate was kept at 75 slpm. Figure 15 plots blue whirl stability against fuel flow rate. Data points shown are for the tangential airflow rates that yielded the greatest stability for each fuel flow rate. The fuel flow rates tested correspond to a heat release rate ranging from 200 to 750 W, assuming complete combustion of the fuel. This upper limit represents a nearly fourfold increase over the heat release rate previously reported by this or any other research group.

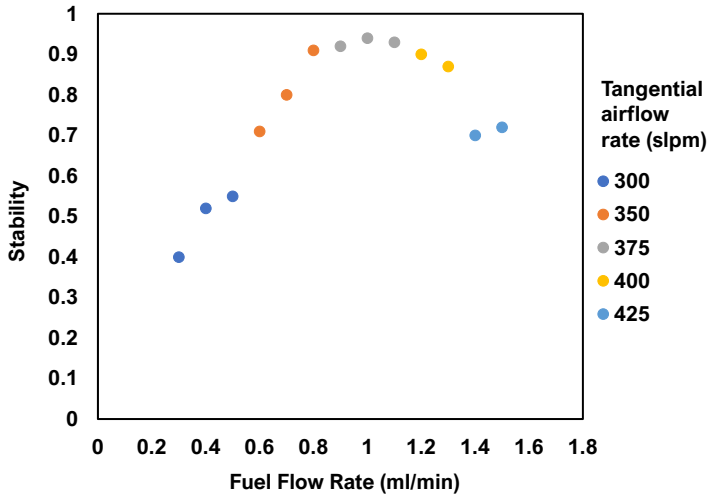

Fig. 15 Stability of n-heptane blue whirls vs. fuel flow rate. Tangential airflow rates shown are those that yielded the most stable flame for each fuel flow rate.

It is clear from Fig. 15 that there is a direct relationship between the fuel flow rate and the tangential airflow required to maintain a stable blue whirl. If we consider the axial velocity of the blue whirl as deriving from buoyancy and therefore from heat release, we can define a dimensionless quantity, $\mathcal{R}^*$, that is analogous to the swirl number in swirling jets. The quantity $\mathcal{R}^*$ may be defined as the ratio of dimensionless circulation to dimensionless heat release rate. Following the non-dimensional analysis used in Hariharan et al.,[17] the most stable blue whirls observed here all possessed a value for $\mathcal{R}^*$ greater than unity. This is consistent with the rotation-dominated flow necessary to maintain the blue whirl structure in the inclined simulations. Here, the increase in blue whirl size was limited only by the onset of turbulence as airflow rates increased.

It is important to note that while much was learned from experimenting with the model fuels mentioned, testing with more complex real fuels was limited. Gasoline was tested in the advanced burner and was seen to form a blue whirl structure, however with greater flicker than the model fuels. It remains to be seen whether this behavior has an impact on the heat release or emissions generated by this fuel.

Other heavier real fuels, such as diesel and JP-8, require heating of the air to vaporize sufficient fuel to reach the lower flammability limit of each. As previously discussed, the advanced burner was designed to accommodate experiments with elevated air temperatures; however, such tests were not performed as part of this study.

3. Conclusions and Recommendations

An investigation was performed at DEVCOM ARL to better understand the fundamentals of the blue whirl, a novel form of combustion that holds promise to form the basis of a fuel-flexible power generation technology. The research identified the essential ingredients needed to form and sustain blue whirls, and determined that the phenomenon was governed primarily by fluid dynamics and fuel properties rather than by chemical kinetics. The blue whirl was successfully simulated, revealing a laminar vortex breakdown flow structure and a confluence of multiple flame types. This structure proved to be robust against rotations up to 15° with respect to gravity. A newly developed burner that provided unprecedented control over experimental inputs was employed to probe the air and fuel flow stability limits of the blue whirl. The burner was able to produce permanently stable blue whirls and scale the thermal output from 200 to 750 W by changing vortex-producing airflows in tandem with fuel flow rates. This relationship held until the onset of turbulence in the airflow.

At the beginning of the project, little was known about the blue whirl other than its surprising discovery and apparent soot-free nature. It was difficult to produce, as few parameters could be controlled beyond fuel flow and air entrainment geometry, and even harder to sustain, as small environmental perturbations would cause flame extinction. Given this starting point, the at-will production and control of blue whirl combustion through the advanced burner and the successful numerical simulation of the blue whirl are the two greatest breakthroughs to come from the present work. These two breakthroughs are what led to the insights into blue whirl stability, scaling, and structure that the project had hoped to deliver.

4. Future Work

The Operational Energy Vision of the Army Futures Command Functional Sustainment Framework calls for energy technologies that extend operational range, mitigate battlefield risk, and are compatible with a hybrid electrification platform. To meet the future needs of a multi-domain Army, one can envision a portfolio approach to energy sourcing in which any number of energy resources that are available to a warfighting unit may be harnessed for power generation. A

single technology capable of producing and utilizing heat from a wide array of energy inputs would therefore be of great benefit. It would comprise two core components: a universal combustor (producing high-grade heat from essentially any fuel) and a universal heat engine (producing power from essentially any heat source). The results of the current project support the candidacy of the blue whirl as a basis for the former; however, much work remains.

We recommend the next research steps focus on developing a blue whirl combustion device that integrates with a heat engine—the Stirling engine being the most likely candidate. Of the many science questions that must be answered to enable this integration, there are two that we deem most critical. The first involves understanding the mechanism of turbulence suppression that accompanies the vortex breakdown event that gives rise to the blue whirl. A laminar flow regime appears to be an essential characteristic of the blue whirl flow structure. This has a direct consequence on the limits to which a single blue whirl flame can be scaled and, therefore, how a combustor must be designed to meet target power outputs. The second question targets a better understanding of the blue whirl's fuel evaporation mechanism. As-constructed, the advanced burner is poised to explore the critical role of incoming air temperature on this mechanism. Results from this investigation would directly impact the heat recuperation design of a practical blue whirl combustor.

5. References

1. ASTM D975-18a. Standard specification for diesel fuel oils. ASTM; 2021 Oct 20.
2. ASTM D4814-18d. Standard specification for automotive spark-ignition engine fuel. ASTM; 2021 Dec 22.
3. Xiao H, Gollner MJ, Oran ES. From fire whirls to blue whirls and combustion with reduced pollution. PNAS. 2016;113(34):9457–9462.
4. Anderson PM, Price L, Gunukula S, Tran DT. Blue whirl phenomenon – a potential fuel-flexible and soot-free combustion technology. Energy & Fuels. 2020;34:11708–11711.
5. Hariharan SB, Anderson PM, Gollner MJ, Oran ES. The blue whirl: boundary layer effects, temperature and OH* measurement. Combustion & Flame. 2019;203:353–361.
6. Dobashi R, Okura T, Nagaoka R, Hayashi Y, Mogi T. Experimental study on flame height and radiant heat of fire whirls. Fire Technology. 2016;52(4):1069–1080.
7. Turns SR. An introduction to combustion: concepts and applications. 2nd ed. McGraw-Hill; 2006.
8. Chung JD, Zhang X, Kaplan CR, Oran ES. The structure of the blue whirl revealed. Science Advances. 2020;33(6).
9. Chung JD, Zhang X, Kaplan CR, Oran ES. The barely implicit correction algorithm for low-Mach-number flows II: application to reactive flows. Computers and Fluids. 2020;210.
10. Zhang X, Chung JD, Kaplan CR, Oran ES. The barely implicit correction algorithm for low-Mach-number flows. Computers and Fluids. 2018;175.
11. Faler JH, Leibovich S. An experimental map of the internal structure of a vortex breakdown. J Fluid Mech. 1978;86:313–335.
12. Zhao D, Gutmark E, de Goey P. A review of cavity-based trapped vortex, ultra-compact, high-g, interturbine combustors. Progress in Energy and Combustion Science. 2018;66:42–82.
13. Dogkas E, Mitsopoulos EP, Koutmos P. Mixing and combustion performance of a stratified bluff body primary zone interacting with a coannular swirl–induced recirculation. Journal of Energy Engineering. 2018;144(4).

14. Chuah KH, Kuwana K, Saito K, Williams FA. Inclined fire whirls. Proceedings of the Combustion Institute. 2011;33:2417–2424.

15. Price LF. Investigating the stability of the blue whirl [master's thesis]. University of Maryland, 2021.

16. Yu D, Zhang P. Circulation-controlled firewhirls with differential diffusion. Combustion & Flame. 2018;189:288–299.

17. Hariharan SB, Hu Y, Gollner MJ, Oran ES. Effects of circulation and buoyancy on the transition from a fire whirl to a blue whirl. Physical Review Fluids. 2020;5.

1 (PDF) DEFENSE TECHNICAL INFORMATION CTR DTIC OCA

1 (PDF) DEVCOM ARL
FCDD RLD DCI
TECH LIB

1 (PDF) DA HQ
DASA(R&T)

9 (PDF) USARMY AFC
L BROUSSEAU
R THYAGARAJAN
A LINZ
K WADE
S BRADY
J REGO
T KELLY
E JOSEPH
B SESSLER

2 (PDF) DEVCOM HQ
FCDD ST
C SAMMS
M HUBBARD

75 (PDF) DEVCOM ARL
FCDD RLC
C BEDELL
B SADLER
T PHAM
B PIEKARSKI
H EVERITT
FCDD RLC CA
L KAPLAN
FCDD RLC ES
G VIDEEN
S HILL
Y PAN
FCDD RLC I
B MACCALL
FCDD RLC N
BM RIVERA
A SWAMI
FCDD RLD
P BAKER
A KOTT
S SILTON
FCDD RLD D
T ROSENBERGER
FCDD RLD E
KS FOSTER
FCDD RLD F
K KAPPRA
FCDD RLD FR
M TSCHOPP
FCDD RLD SM
L BLUM
FCDD RLH
J CHEN
PJ FRANASZCZUK
C LANE
K MCDOWELL
FCDD RLH B
JJ SUMNER
FCDD RLH F
JR GASTON
FCDD RLH T
D STRATIS-CULLUM
FCDD RLL
T KINES
FCDD RLL D
J S ADAMS
FCDD RLL DP
J MCCLURE
FCDD RLR
B HALPERN
S LEE
D STEPP
FCDD RLR E
RA MANTZ
C VARANASI
FCDD RLR EL
JX QIU
MD ULRICH
FCDD RLR EN
RA ANTHENIEN JR
FCDD RLR IC
MA FIELDS
SP IYER
FCDD RLR IM
JD MYERS
FCDD RLR IN
XN WANG
FCDD RLR
P REYNOLDS
FCDD RLR P
LL TROYER
FCDD RLR PC
D POREE
FCDD RLR PL
MK STRAND
FCDD RLS
J ALEXANDER
M GOVONI
M WRABACK
FCDD RLS C
M REED
FCDD RLS CC
P ANDERSON
S BEDAIR

FCDD RLS CE
TR JOW
K XU
FCDD RLS CL
M DUBINSKIY
FCDD RLS E
RD DELROSARIO
FCDD RLS ED
K JONES
FCDD RLS EA
A ZAGHLOUL
FCDD RLS S
WL BENARD
FCDD RLS SO
W ZHOU
FCDD RLW
S KARNA
JF NEWILL
AM RAWLETT
SE SCHOENFELD
J ZABINSKI
FCDD RLW B
R BECKER
FCDD RLW M
ES CHIN
FCDD RLW S
V CHAMPAGNE
AL WEST
FCDD RLW T
RZ FRANCART
FCDD RLW TC
JD CLAYTON
FCDD RLW W
TV SHEPPARD
FCDD RLW WA
B RICE
R PESCE-RODRIGUEZ
FCDD RLW M
A HALL